ARTICLE

Influences of Current Density on Tribological Characteristics of Ceramic Coatings on ZK60 Mg Alloy by Plasma Electrolytic Oxidation

Xiaohong Wu,[†] Peibo Su,[‡] Zhaohua Jiang,*[,‡] and Song Meng[§]

Department of Chemistry and School of Chemical Engineering and Technology, Harbin Institute of Technology, Harbin 150001, P.R. China, and China Academy of Space Technology, Beijing 100094, P.R. China

ABSTRACT Current density is a key factor of plasma electrolytic oxidation process. Its influences on structure, mechanical, and tribological characteristics of ceramic coatings on ZK60 Mg alloy by pulsed bipolar microplasma oxidation in Na_3PO_4 solution were studied in this paper. Thickness, structure, composition, mechanical property, and tribological characteristics of the coatings were studied by eddy current coating thickness gauge, scanning electron microscope (SEM), X-ray diffraction (XRD), nanoindentation measurements, and ball-on-disk friction testing. The results show that all the coatings prepared under different current densities are composed of MgO phase. The amount of MgO phase, thickness and friction coefficient of the coatings increased with the increasing current density. Among three ceramic coatings produced under three current densities, the coating produced under the current density of 7 A/dm^2 got the highest nanohardness and lowest wear rate with the value of 1.7 GPa and 1.27 × 10^{-5} mm^3/Nm.

KEYWORDS: plasma electrolytic oxidation • ceramic coatings • tribological characteristic • mg alloy

1. INTRODUCTION

As reported, the strength of ZK60 Mg alloy is the highest of the commercial magnesium alloys (1). Furthermore, because of the lightweight of Mg alloy, ZK60 Mg alloy has the highest strength to weight ratio of all those metals. However, the main factors of their limited application are their comparatively low corrosion and wear resistance (2). Plasma electrolytic oxidation (PEO), also called as micro plasma oxidation (MPO) or micro arc oxidation (MAO), and a new surface treatment technology developed recently, has become a hotspot of international researches (3−5). It removes the drawbacks of the conventional anodic oxidation operating voltage. Because of the introduction of the work zone into the high-voltage discharge zone, ceramic coating is directly formed on the surface of substrates such as Al, Ti, Mg, etc., with the high instant temperature in the micro zone. Through PEO, in situ grown ceramic coating is directly formed on the surface of substrate, which can remarkably enhance the surface properties of metals, such as wear resistance, corrosion resistance, and especially adhesion for post coats (6, 7).

So far, most research has focused on the electrochemical corrosion behavior of PEO technique on Mg alloy (8−11). The tribological characteristics of PEO coatings formed on Mg alloys are seldom studied (12−14). In this study, influences of current density on the structure, mechanical and tribological characteristics of ceramic coatings on ZK60 Mg alloy by PEO are researched.

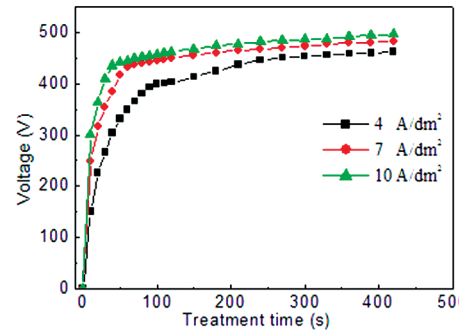

FIGURE 1. Voltage−time response for PEO coatings produced under different current densities.

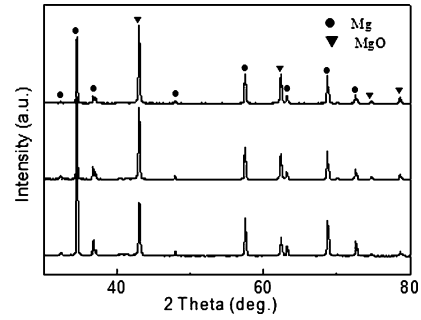

FIGURE 2. XRD patterns of the ceramic coatings produced under different current densities: (a) 4, (b) 7, (c) 10 A/dm^2.

2. EXPERIMENTAL SECTION

2.1. Preparation of PEO Coatings. Polished rectangular sample (with dimensions 25 mm × 20 mm × 2 mm) made of ZK60 Mg alloy (mass fraction: Zn 5.5%, Zr 0.5%, balance Mg) was used as the substrate material in this study. Before PEO treatment, every surface of magnesium samples was succes-

* Corresponding author. Phone: 086-0451-86402522. Fax: 086-0451-86402522. E-mail: wxhqw@263.net.

Received for review November 19, 2009 and accepted February 1, 2010

† Department of Chemistry, Harbin Institute of Technology.

‡ School of Chemical Engineering and Technology, Harbin Institute of Technology.

§ China Academy of Space Technology.

DOI: 10.1021/am900802x

Published on Web 02/22/2010

sively ground down to 1000# SiC papers, and then respectively ultrasonic degreased in ethanol and distilled water. A home-made pulsed bipolar electrical source with power of 5 kW was used for plasma electrolytic oxidation of samples in a water-cooled electrobath made of stainless steel, which also served as the counter electrode. The reaction temperature was controlled below 30 °C with a cooling water flow. The PEO process equipment used is similar to the one presented by Matthews' group (6). An aqueous electrolyte was prepared from a solution of sodium phosphate (8 g/L), potassium hydroxide (3 g/L) and sodium fluoride (1 g/L). The electronic power frequency was fixed at 1000 Hz. The duty ratios of both pulses were both equal to 45%. The whole process was carried out for 7 min under the current density of 4, 7, and 10 A/dm^2, respectively. After PEO treatment, the coated samples were rinsed with water and dried in the air.

Table 1. Average Thickness of the PEO Coatings Produced under Different Current Densities

I (A/dm^2)	4	7	10
mean thickness (μm)	16.7	22.6	27.9

2.2. Analysis of Composition and Structure of PEO Coatings. The phase composition of the coating was examined with X-ray diffraction (XRD), using a Cu Kα source. The surface and cross-section morphology of the prepared coating was studied with scanning electron microscopy (SEM; Hitachi S-570).

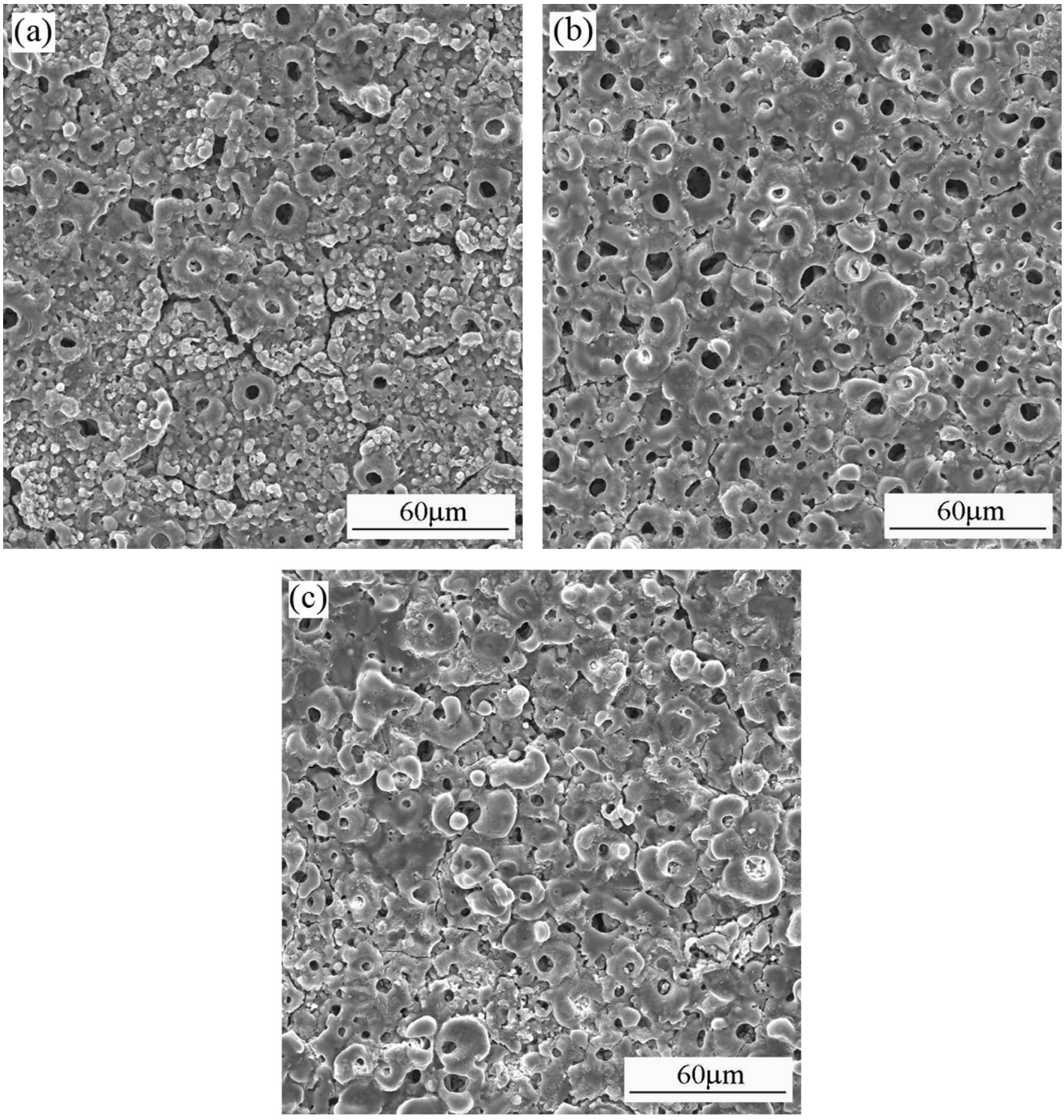

FIGURE 3. Surface morphologies of the ceramic coatings produced under different current densities: (a) 4, (b) 7, (c) 10 A/dm^2.

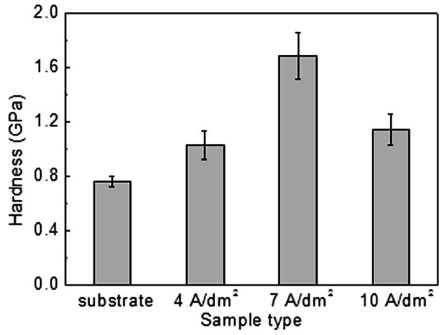

FIGURE 4. Nanohardess of the surface of the Mg alloy substrate and ceramic coatings produced under different current densities.

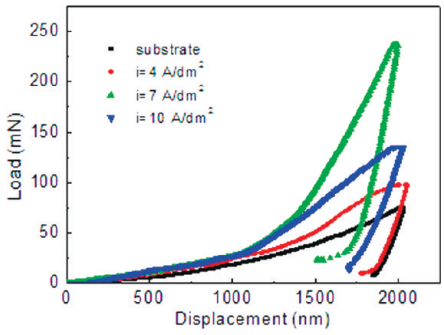

FIGURE 5. Typical load−displacement curves for the substrate and ceramic coatings produced under different current densities.

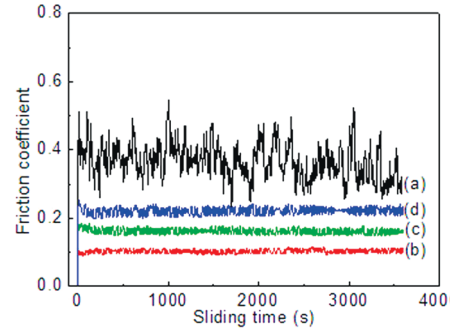

FIGURE 6. Friction coefficients of the substrate and ceramic coatings produced under different current densities: (a) substrate, (b) 4, (c), (d) 10 A/dm^2.

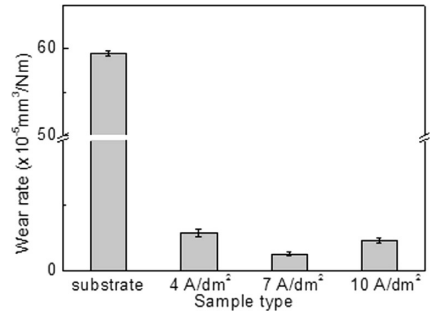

FIGURE 7. Wear rates of the substrate and ceramic coatings produced under different current densities.

The coating thickness was measured, using an eddy current-based thickness gauge (CTG-10, Time Company, China) with a minimum resolution of 1 μm and accuracy of 0.1 μm. In this experiment, the average thickness of each sample was obtained from 10 measurements at different positions.

2.3. Mechanical and Tribological Evaluation. Nanoindentation was performed on a nanoindenter XP (Nano Instruments, MTS Systems Corporation, USA) with a Berkovich diamond indenter. All of the measurements were made with 2 μm penetration depth. The elastic modulus and hardness values were derived from the load−displacement curves using the method of Oliver and Pharr (15). Typically 5 indents were obtained for individual specimens, from which average values were calculated. The wear experiments were performed on ball-on-disk tribometer (Center for Tribology, HIT, China) with a 52100 steel ball of 10 mm diameter as friction partner at ambient temperature and humidity. The normal load was 2 N, and the sliding speed was 0.10 m/s. The total sliding time was 4 h. The friction coefficients were recorded automatically during the test process. After the test, the wear rates of the samples were calculated by measuring the cross-sectional area of worn scar of the sample with a profilometer. The wear track of the samples were observed by SEM.

3. RESULTS AND DISCUSSION

3.1. Voltage−Time Response. After the PEO process began, the current density was kept constant at a certain value, whereas the instantaneous variation of voltage was recorded every 10 s before the first 2 min and every 30 s after 2 min. The galvanostatic dependencies of positive voltage on PEO treatment time obtained under different current density are shown in Figure 1, in which the current density is 4, 7, and 10 A/dm^2, respectively. As shown in Figure 1, the positive voltage increased as the current density increased. From the commencement of anodizing, the voltage increased approximately linearly with time to ~300 at 6 V/s. Subsequently, the slopes reduced. The raise of the voltage increased slowly from 2 to 7 min. The color of the microdischarges changed from blue-white at the voltage of 200 V to orange at the voltage of 350 V. Table 1 reports the measurements of the average coatings thickness under different current density. As shown in Table 1, it is clear that the average coating thickness increases as the applied current density increases.

3.2. Phase Composition of the Coatings. XRD spectra of the surface layers in Figure 2a−c show the phase composition of PEO coatings prepared in the same electrolyte changes substantially with the variations of the current densities. Obviously, no matter what the current density was, the coating was invariably composed of MgO. The relative content of MgO increased as the current density increased, which could be attributed to the thicker thickness of the coatings.

3.3. Morphologies of the Coatings. Surface morphologies of PEO coatings produced under different current densities are observed by SEM (Figure 3). As shown in Figure 3, there are many micropores and some microcracks on surfaces of these PEO coatings. Micropores were formed by molten oxide and gas bubbles thrown out of microarc discharge channels (16, 17), whereas microcracks were caused by thermal stress due to rapid solidification of molten oxide in the relatively cool electrolyte. Moreover, the lower Pilling-Bedworth ratio (PBR) of magnesia (PBR of a metal oxide is defined as the ratio of the volume of the metal oxide to the consumed metal volume) is also the main reason for high porosity of PEO films on magnesium alloys (18). In Figure 3, the micrographs clearly indicate the presence of discharge channels appearing as dark circular spots distrib-

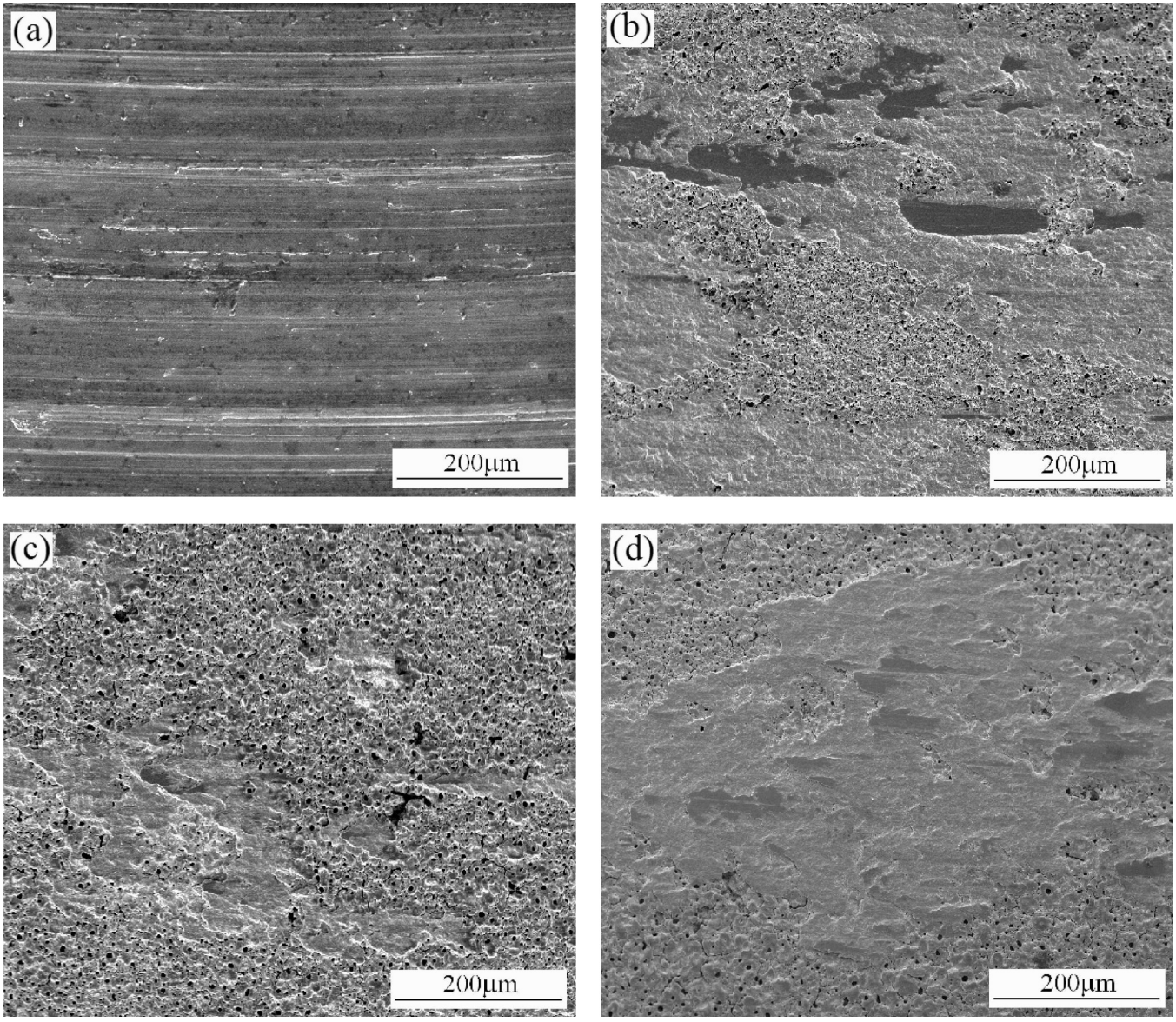

FIGURE 8. SEM micrographs of wear tracks of the substrate and ceramic coatings produced under different current densities: (a) substrate, (b) 4, (c) 7, (d) 10 A/dm^2.

uted all over the surface of the coatings. It is also apparent that the number of the channels and the discharge channel diameter increase with increasing current density when the current density is 4 and 7 A/dm^2. Then both of them decrease with increasing current density when the current density is 7 and 10 A/dm^2. The increasing current density leads to an enhanced discharging energy, hence the increased product mass by a single pulse, which contributes to the enlarged pore sizes after the discharged channels are cooled. As the discharge intensity increases continuously, the accumulated production mass of oxide increases, which induces a gradually increasing grain size and overlaps the pores nearby.

3.4. Mechanical and Tribological Performance. ***3.4.1. Nanoindentation Measurements.*** Figure 4 shows the nanohardness of surface of Mg alloy substrate and samples produced under different current densities. It can be seen that after PEO treatment, the nanohardness increased because of the formation of ceramic PEO coatings on magnesium alloy ZK60 substrate. The nanohardness reached the highest when the current density was fixed at 7 A/dm^2, which was 1.7 GPa. The increasing current density leads to an increase in MgO phase, which could enhance the hardness. As the current intensity increases continuously, the surface of the sample turned to lose. So the nanohardness decreased when the current density reached up to 10 A/dm^2. Figure 5 shows the load−displacement curves registered for the Mg alloy substrate and samples produced under different current densities. The maximum displacement results from elastic and plastic deformation, with elastic recovery occurring on unloading. The loads applied to reach the same penetration depth of 2000 nm were 70, 100, 235, and 135 mN for the substrate and the coatings produced under the current density of 4, 7, and 10 A/dm^2, respectively. The elastic recovery of the coatings was 11.3, 24.6, and 15% when the current density was fixed at 4, 7, and 10 A/dm^2, respectively,

which was higher than that of the substrate, i.e., 7.7%. The elastic modulus of the substrate and coatings produced under the current density of 4, 7, and 10 A/dm^2 were 44, 54, 90, and 60 GPa, respectively.

3.4.2. Tribological Properties. The typical evolution of friction coefficient with sliding time for Mg alloy substrate and the PEO coatings produced under the current density of 4, 7, and 10 A/dm^2 is shown in Figure 6. For the uncoated Mg alloy substrate, the friction coefficient varies in the range of 0.2−0.5, accompanied by severe oscillation (curve a in Figure 6). The oscillation of friction coefficient demonstrates that the Mg alloy substrate shows poor tribological behavior without a protective surface coating. Curves b, c, and d in Figure 6 show improved tribological behavior provided by the PEO coating, which was characterized by stable and steady state condition in the long-term wear testing. The average friction coefficient of the coated samples produced under the current density of 4, 7, and 10 A/dm^2 were about 0.10, 0.16, and 0.22, respectively. The differences of friction coefficient of the coated samples could be attributed to the increased roughness as the current density increased.

Figure 7 shows the wear rates of the uncoated Mg alloy substrate and the PEO coatings produced under the current density of 4, 7, and 10 A/dm^2. The uncoated Mg alloy substrate has a high wear rate of 5.94×10^{-4} mm^3/Nm, whereas the wear rates of the three coated samples are only in the range of $1.27-2.90 \times 10^{-5}$ mm^3/Nm. This indicates that the PEO coatings have much better wear resistance than the Mg alloy substrate. Furthermore, the sample produced under the current density of 7 A/dm^2 has a better wear resistance than the other samples, though the sample of 7 A/dm^2 has a higher friction coefficient than that of 4 A/dm^2 during the sliding time. The enhancement of the wear resistance is probably due to the more compact structure and higher hardness of the coating prepared under the current density of 7 A/dm^2.

The micrographs of the wear tracks of the uncoated Mg alloy substrate and the PEO coatings, examined in SEM, are presented in Figure 8. It could be seen that the worn surface of the uncoated Mg alloy was characterized by typical features of adhesive and abrasive wear, with evident grooves and ploughs paralleling to the sliding direction (Figure 8a). In the case of the PEO coatings, the wear tracks showed many noncontinuous cracks and the worn area was smaller and shallower than that of the Mg alloy, which indicated that the coatings seemed to have provided the resistance to the magnesium substrate against adhesive wear. The appearance of the corresponding wear tracks on the PEO coating produced under the current density of 7 A/dm^2 was more intact than that of the other two coatings. In the circumstance of 4 A/dm^2, some parts of the outer porous layer were scratched out during the sliding. As the coating of 10 A/dm^2, the out loose layer was rubbed down to smooth and the pores of the coating were filled up. All these demonstrate that the coating of 7 A/dm^2 has higher resistance to adhesive wear than the other two kind of coatings and the magnesium alloy substrate because the roughness especially the hardness of the coatings seem to have played a crucial role in the wear process.

4. CONCLUSION

MgO coatings were formed on the surface of ZK60 magnesium alloy using the plasma electrolytic oxidation technique. The current density has influenced the morphology, hardness, and wear resistance of the coatings, which is a key technique parameter in the PEO process. The wear resistance of the magnesium alloy is significantly improved by PEO coatings on the surface. The wear rates of the PEO coatings were around 10 times lower than that of the uncoated Mg alloy substrate. The coating prepared under the current density of 7 A/dm^2 exhibited higher nanohardness, relatively lower friction coefficient and higher wear resistance than the other two kinds of coatings prepared under the current density of 4 and 10 A/dm^2.

Acknowledgment. The authors thank the National key Laboratory of Vacuum and Cryogenics Technology and Physics (Project 9140C550201060C55) for the financial support for this work.

REFERENCES AND NOTES

(1) Bussiba, A.; Ben, A. A.; Shtechman, A.; Ifergan, S.; Kupiec, M. *Mater. Sci. Eng., A* **2001**, *302*, 56–62.
(2) Yamauchi, N.; Demizu, K.; Ueda, N.; Cuong, N. K.; Sone, T.; Hirose, Y. *Surf. Coat. Technol.* **2005**, *193*, 277–282.
(3) Wirtz, G. P.; Brown, S. D.; Kriven, W. M. *Mater. Manuf. Process* **1991**, *6*, 87–115.
(4) Kurze, P. *Metalloberflache* **1994**, *48*, 104–105.
(5) Zozulin, A. J.; Bartak, D. E. *Met. Finish.* **1994**, *92*, 39–44.
(6) Yerokhin, A. L.; Nie, X.; Leyland, A.; Matthews, A.; Dowey, S. J. *Surf. Coat. Technol.* **1999**, *122*, 73–93.
(7) Lv, G. H.; Gu, W. C.; Chen, H.; Feng, W. R.; Khosa, M. L.; Li, L.; Niu, E.; Zhang, G. L.; Yang, S. Z. *Appl. Surf. Sci.* **2006**, *253*, 2947–2952.
(8) Lv, G. H.; Chen, H.; Gu, W. C.; Li, L.; Niu, E. W.; Zhang, X. H.; Yang, S. Z. J. *Mater. Process. Technol.* **2008**, *208*, 9–13.
(9) Bala Srinivasan, P.; Blawert, C.; Dietzel, W. *Mater. Sci. Eng., A* **2008**, *494*, 401–406.
(10) Luo, H. H.; Cai, Q. Z.; Wei, B. K.; Yu, B.; Li, D. J.; He, J.; Liu, Z. *J. Alloys Compd.* **2008**, *464*, 537–543.
(11) Ghasemi, A.; Raja, V. S.; Blawert, C.; Dietzel, W.; Kainer, K. U. *Surf. Coat. Technol.* **2008**, *202*, 3513–3518.
(12) Liang, J.; Hu, L. T.; Hao, J. C. *Appl. Surf. Sci.* **2007**, *253*, 4490–4496.
(13) Liang, J.; Guo, B. G.; Tian, J.; Liu, H. W.; Zhou, J. F.; Xu, T. *Appl. Surf. Sci.* **2005**, *252*, 345–351.
(14) Jin, F. Y.; Chu, P. K.; Xu, G. D.; Zhao, J.; Tang, D. L.; Tong, H. H. *Mater. Sci. Eng., A* **2006**, 435–436, 123−126.
(15) Oliver, W. C.; Pharr, G. M. *J. Mater. Res.* **1992**, *7*, 1564–1583.
(16) Guo, H. F.; An, M. Z. *Appl. Surf. Sci.* **2005**, *246*, 229–238.
(17) Sharma, A. K.; Uma Rani, R.; Malek, A.; Acharya, K. S. N.; Muddu, M.; Kumar, S. *Met. Finish.* **1996**, *94*, 16–27.
(18) Zhou, X.; Thompson, G. E.; Skeldon, P.; Wood, G. C.; Shimizu, K.; Habazaki, H. *Corros. Sci.* **1999**, *41*, 1599–1613.

AM900802X